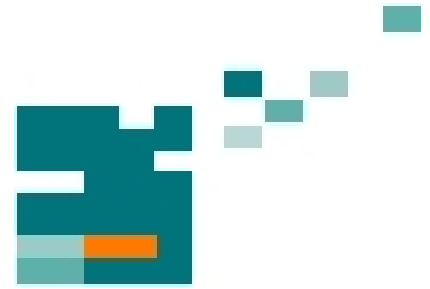


54. IWK
Internationales Wissenschaftliches Kolloquium
International Scientific Colloquium



**Information Technology and Electrical
Engineering - Devices and Systems, Materials
and Technologies for the Future**



Faculty of Electrical Engineering and
Information Technology

Startseite / Index:

<http://www.db-thueringen.de/servlets/DocumentServlet?id=14089>

Impressum

Herausgeber: Der Rektor der Technischen Universität Ilmenau
Univ.-Prof. Dr. rer. nat. habil. Dr. h. c. Prof. h. c.
Peter Scharff

Redaktion: Referat Marketing
Andrea Schneider

Fakultät für Elektrotechnik und Informationstechnik
Univ.-Prof. Dr.-Ing. Frank Berger

Redaktionsschluss: 17. August 2009

Technische Realisierung (USB-Flash-Ausgabe):
Institut für Medientechnik an der TU Ilmenau
Dipl.-Ing. Christian Weigel
Dipl.-Ing. Helge Drumm

Technische Realisierung (Online-Ausgabe):
Universitätsbibliothek Ilmenau
[ilmedia](#)
Postfach 10 05 65
98684 Ilmenau

Verlag:



Verlag ISLE, Betriebsstätte des ISLE e.V.
Werner-von-Siemens-Str. 16
98693 Ilmenau

© Technische Universität Ilmenau (Thür.) 2009

Diese Publikationen und alle in ihr enthaltenen Beiträge und Abbildungen sind urheberrechtlich geschützt.

ISBN (USB-Flash-Ausgabe): 978-3-938843-45-1
ISBN (Druckausgabe der Kurzfassungen): 978-3-938843-44-4

Startseite / Index:

<http://www.db-thueringen.de/servlets/DocumentServlet?id=14089>

CONTRIBUTION TO THE APPLICATION OF THE SOLA-VOF METHOD FOR MFD FLOWS

Ovidiu Peşteanu

Department of Electrical Engineering, Transilvania University of Braşov,
B-dul Eroilor 29, 900036 Braşov, Romania

ABSTRACT

The paper presents a strictly volume conserving VOF method combined with a local height function, developed for the numerical simulation of MFD free surface flows. Near the free surface, the variable space-distribution of the Lorentz forces is considered by a proper computation of the electromagnetic field and pressure. After every calculation time step, the transient free surface is reconstructed using line segments of three orientation types, on which accurate stress conditions can be applied. The calculated free surface of Wood's metal in a laboratory induction furnace shows a good agreement with the measurements.

Index Terms – Free surface flow, finite difference method, VOF method, generalized local height function, pressure at melt free surface in electromagnetic field, three-line interface construction

1. INTRODUCTION

One of the widely used methods for the treatment of unsteady free surfaces is the Volume Of Fluid (VOF) method based on the advection of a VOF function F [1] indicating the fractional volume of a computational cell filled with fluid, i.e. $F = 0$ in the empty cells E (Fig. 1), $0 < F < 1$ in the adjacent surface cells S containing free surface sections, and $0 < F \leq 1$ in the other remaining fluid cells F, respectively.

The pressure in an S cell is calculated as a linear interpolation (or extrapolation) between the pressure in an adjacent F cell and the pressure at the free surface [1, 2]. The thus obtained values are accurate for flows driven by constant force densities, but could be inaccurate for the MagnetoFluidDynamic (MFD) flows driven by variable electromagnetic force densities, increasing toward the free surfaces of the molten metals.

After every calculation time step, the free surface is reconstructed using either a Simple Line Interface Construction (SLIC) [1, 3] or a more accurate method employing a Piecewise Linear Interface Construction (PLIC) [4–6].

The applying of the donor-acceptor [1] and PLIC methods [4, 5] can yield values $F < 0$ or $F > 1$ and by their rounding to 0 and 1, respectively, the volume of an incompressible fluid is no more conserved.

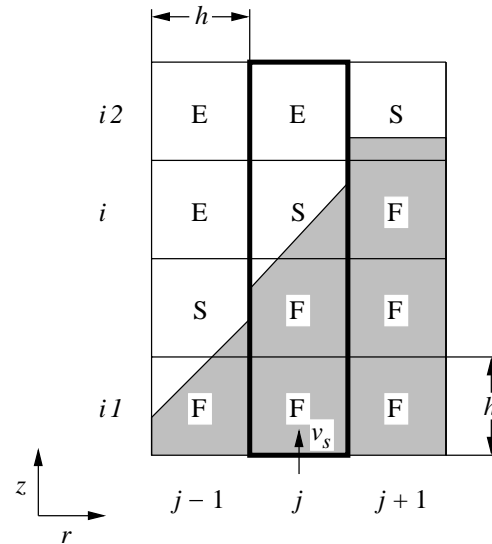


Fig. 1. Cell labels and column for defining the LHF.

For a rigorous volume conserving and to prevent the numerical creation of unphysical holes and droplets separated from the main body of fluid, the VOF method was combined with a Local Height Function (LHF) [7] using a SLIC of the free surface, and successfully employed e.g. in the simulation of coupled liquid-solid dynamics in spacecraft [8] and of water waves impact problems [9, 10], respectively.

In this paper the VOF method is extended to the simulation of electromagnetically driven free surface flows by the followings:

- Proper calculation of the electromagnetic field and pressure in S cells considering the variable space-distribution of Lorentz forces
- Volume conserving displacement of free surface by applying a VOF method combined with a generalized LHF
- Three-Line Interface Construction (TLIC), i.e. the free surface is reconstructed using three types of line segments: horizontal, vertical and inclined at 45° , on which accurate stress boundary conditions can be employed

By using the Finite Difference Method (FDM), the proposed MFD LHF-VOF method was applied for the modeling of the turbulent molten metal flow in an Induction Crucible Furnace (ICF) [11], the calculated free surface form showing a good agreement with the measurements presented in [12].

2. FREE SURFACE APPROXIMATION

The free surface boundary conditions for the velocity \mathbf{v} and pressure p_s are given by [2, 8–10]

$$\begin{aligned} \frac{\partial v_n}{\partial \mathbf{t}} + \frac{\partial v_t}{\partial \mathbf{n}} &= 0, \\ p_s &= p_a + p_\gamma + 2\mu_{\text{eff}} \frac{\partial v_n}{\partial \mathbf{n}}, \end{aligned} \quad (1)$$

where v_n and v_t are the normal and tangential velocities, p_a is the ambient pressure, p_γ denotes the pressure due to the surface tension γ and μ_{eff} represents the effective viscosity.

For an arbitrary orientation of the free surface, the application of the stress conditions (1) yields complicate equations [13]. Simple equations, representing accurate boundary conditions, can be obtained by the Eqs. (1) e.g. for the following three local orientations of the upper surface of an axisymmetric flow with the velocities u and v in the r - and z -directions [2, 14]:

Horizontal orientation

$$\frac{\partial v}{\partial r} + \frac{\partial u}{\partial z} = 0, \quad \frac{\partial v_n}{\partial \mathbf{n}} = \frac{\partial v}{\partial z}. \quad (2)$$

Vertical orientation

$$\frac{\partial u}{\partial z} + \frac{\partial v}{\partial r} = 0, \quad \frac{\partial v_n}{\partial \mathbf{n}} = \frac{\partial u}{\partial r}. \quad (3)$$

Inclined orientation at 45°

$$\frac{\partial u}{\partial r} - \frac{\partial v}{\partial z} = 0, \quad \frac{\partial v_n}{\partial \mathbf{n}} = \pm \frac{1}{2} \left(\frac{\partial u}{\partial z} + \frac{\partial v}{\partial r} \right), \quad (4)$$

where the sign is ‘+’ for a decreasing surface level in radial direction, and ‘-’ for an increasing one, respectively [14].

Due to the accuracy of conditions (2)–(4), only the three corresponding types of line segments will be chosen for the free surface reconstruction in this study. By using this TLIC, the method is more accurate than the algorithms using a SLIC and more simple than the methods based on the PLIC.

3. CALCULATION OF THE MFD FIELD

The free surface is reconstructed in two steps (**Fig. 2**):

- First by a SLIC (Fig. 2 left), for the electromagnetic field and turbulent flow computation
- Then, by the more accurate TLIC (Fig. 2 right), for its displacement by the LHF-VOF method

3.1. Electromagnetic field computation

The electromagnetic field is calculated considering all F and S cells, resulted from a SLIC of the free surface (Fig 2 left) as being completely filled, i.e. by using in all these cells the electrical conductivity σ of the melt.

The use of a reduced conductivity, e.g. $F\sigma < \sigma$ in the cells with $F < 1$, yields lower Lorentz forces driving unrealistic, too weak near-surface tangential flows, and as a result, a wrong form of the free surface can be calculated, as presented in Sect. 6.

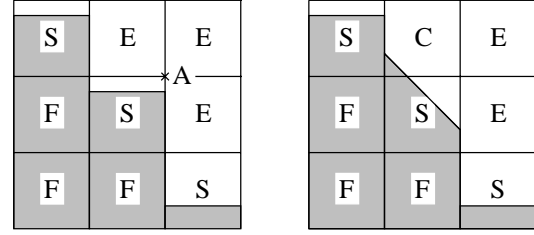


Fig. 2. Successive recalculations of the free surface.

3.2. Calculation of turbulent flow

An unsteady flow is modeled by solving the FF, FS and SS momentum equations [8–10] and the turbulence field equations in the F and S cells, e.g. the transport equations of k and ε , considering that all F and S cells are completely filled with melt.

In a new S cell appeared in a transient modeling, the turbulence field quantities from a neighboring cell chosen in the direction most normal to the free surface, are set as initial values, e.g. the values of k , ε and μ_{eff} , respectively.

3.3. Velocity at the free surface

Beside the stress conditions (2)–(4), in all S cells the continuity equation

$$\frac{1}{r} \frac{\partial}{\partial r} (ru) + \frac{\partial v}{\partial z} = 0 \quad (5)$$

is used because of the following reasons:

- If instead of Eq. (5) another condition is employed, e.g. a constant or linear extrapolation of the tangential velocity [9, 10], then, when an S cell with $\text{div } \mathbf{v} \neq 0$ changes to an F cell with $\text{div } \mathbf{v} = 0$, numerical spikes occur in the pressure field [10]
- When using the k - ε or the Reynolds stress model, the production terms are physically more accurately computed in those S cells, where the continuity equation was used

For example, Eq. (5) together with the tangential stress condition from Eqs. (4) yield the following equations for calculation of the boundary S-velocities on a 45° inclined surface section

$$\frac{1}{r} \frac{\partial}{\partial r} (ru) + \frac{\partial u}{\partial r} = 0, \quad \frac{\partial v}{\partial z} = \frac{\partial u}{\partial r}. \quad (6)$$

In an S cell with two neighboring E cells not positioned opposite each other, the volume conservation in direction most normal to the free surface is additionally demanded [8].

Other boundary values of velocity, needed for the calculation of turbulence production terms, can be determined by the equations representing constant extrapolations of the velocity components along their normal directions [14]

$$\frac{\partial u}{\partial z} = 0, \quad \frac{\partial v}{\partial r} = 0, \quad (7)$$

discretised for the central points of every 2×2 block comprising an S cell and three E cells, e.g. for the point A in Fig. 2 left.

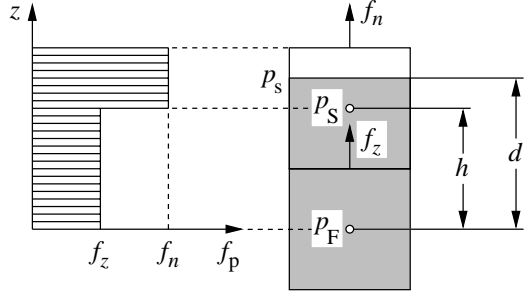


Fig. 3. Concerning the pressure calculation in S cells.

3.4. Pressure at the free surface

In applying the FDM, the variable potential component f_p of the vertical force density in an electromagnetic field can be assumed to be piecewise constant (**Fig. 3** left). If the free surface lies in **Fig. 3** right between the central points of the neighboring F and S cells, i.e. if $d \leq h$, then the pressures at the free surface and in the S cell can be written as

$$p_s = p_F + f_z d, \quad p_S = p_F + f_z h, \quad (8)$$

and after elimination of f_z , one obtains the known extrapolated pressure [1, 2]

$$p_S = \eta p_s + (1 - \eta) p_F \quad \text{if } d \leq h, \quad (9)$$

where $\eta = \frac{d}{h}$ is determined with the distance d from the free surface geometry resulted after the surface reconstruction by a SLIC.

For $d > h$, the pressure in an S cell can be more accurately calculated by the normal force density acting on the outer face of the cell considered completely filled with melt (**Fig. 3** right)

$$p_S = p_s - f_n(d - h) \quad \text{if } d > h. \quad (10)$$

Thus, the surface force density $f_n \neq f_z$ not used in the momentum equations can be taken into account in the pressure calculation, too.

3.5. Velocity and pressure correction

For every computational time step, after calculating all FF, FS and SS velocities by the momentum equations, either the Poisson equation for the pressure is solved or the SOLution Algorithm (SOLA) [1, 15] is applied for the correction of pressure and velocity in order to satisfy continuity.

As the continuity Eq. (5) was utilized in all S cells, and the S-pressures were obtained according to the Eqs. (9) and (10), the Poisson equation or the iterative SOLA code are used only for the F cells.

4. FREE SURFACE DISPLACEMENT

4.1. The generalized LHF

When using an uniform grid, a generalized LHF H corresponding to every S cell i, j (**Fig. 1**) is determined as in [7–10] by adding the VOF fractions in a multi-cell block comprising $N \geq 3$ cells, chosen in the direction most normal to the free surface:

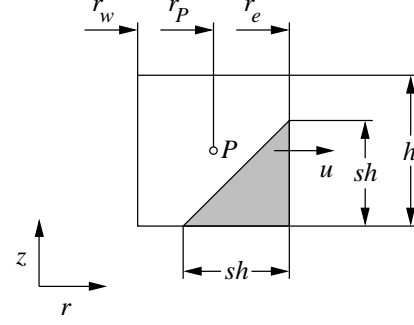


Fig. 4. Inclined section of free surface in an S cell.

$$H_j = \sum_m F_{m,j}, \quad (11)$$

in which the summation is from the lowest $m = i1$ to the uppermost $m = i2$ row of three cells, containing at least a partly filled cell, i.e. the three cells $j - 1, j$ and $j + 1$ below $i1$ are F and above $i2$ E cells, respectively.

Because the computational cells have in r -direction different volumes depending on their mean radii r_j , the generalized LHF is calculated in radial direction by a radius-averaging as:

$$H_i = \frac{1}{R} \sum_n r_n F_{i,n}, \quad R = \frac{1}{N} \sum_n r_n, \quad (12)$$

where the summations are from $n = j1$ to $n = j2$, $j1$ and $j2$ being defined in r -direction in a similar manner as $i1$ and $i2$ in z -direction, while $N = j2 - j1 + 1$.

In z -direction and for $N = 3$, the generalized LHF becomes the usual LHF used in [7–10].

4.2. Local conservation of melt volume

The free surface advection will be briefly presented for the upper surface of an axisymmetric flow, too.

The conservation of fluid volume in a multi-cell block during a computational time step Δt , e.g. in the vertical thick line column in **Fig. 1**, may be expressed by the explicit discretisation equation

$$(H_j^{\text{new}} - H_j) V_j + \sum_m (V_{em} - V_{wm}) - V_s = 0, \quad (13)$$

$$V_j = 2\pi r_j h^2, \quad V_s = 2\pi r_j v_s \Delta t h,$$






where V_j is the volume corresponding to the cell i, j , V_{em} and V_{wm} indicate the molten metal volumes convected through the eastern and western faces of cell m, j , which can be determined by the outward fluxes across the lateral cell faces, and v_s denotes the velocity across the southern side of the cell block (**Fig. 1**).

An outward flux convected during Δt through the right face of the cell shown in **Fig. 4**, calculated by the fraction s of the two cell sides located within the melt and by the outgoing velocity u across the right side, respectively, results as [4]

$$V_r = 2\pi r_e \frac{(sh)^2 - (sh - u \Delta t)^2}{2} \quad \text{if } u \Delta t \leq sh, \quad (14)$$

$$V_r = 2\pi r_e \frac{(sh)^2}{2} = 2\pi r_p F h^2 \quad \text{if } u \Delta t > sh.$$

Table 1. Calculation of dimensionless fluxes Φ across the right cell face when $0 \leq q \leq 1$.

Case	q	Φ
		qF
I 	$\leq s$	$qs - q^2/2$
	$> s$	λF
II 	$\leq s$	q
	$> s$	$q - (q - s)^2/2$
III 	$\leq 1 - s$	0
	$> 1 - s$	$(q + s - 1)^2/2$
IV 	$\leq 1 - s$	$qs + q^2/2$
	$> 1 - s$	$q - \lambda(1 - F)$

Following the same calculation stencil and defining the nondimensional variables

$$q = \frac{u \Delta t}{h}, \quad \Phi = \frac{V_r}{2\pi r_e h^2}, \quad \lambda = \frac{r_p}{r_e}, \quad (15)$$

one obtains the dimensionless outward fluxes Φ across the right cell side summarized in **Table 1** for different possible configurations, where s denotes the fraction of cell sides lying within the melt.

The outward fluxes through the left cell side can be determined replacing r_e by r_w in the nondimensionalization Eqs. (15) and using for the cases I, II, III and IV the values of Φ given in Table 1 for the cases III, IV, I and II, respectively.

In calculation of the volumes convected through the faces of the supplementary appeared cells after the free surface TLIC, e.g. the cell C in Fig. 2 right, the velocities obtained by applying the free surface stress conditions for the neighboring S cells can be used.

5. FREE SURFACE RECONSTRUCTION

By employing a stability limited time step in Eqs. (13), no undershoots $H < 0$ or overshoots $H > N$ can appear for the generalized LHF of the N -cell blocks and as a result, the method is strictly mass conserving. The individual VOF fractions F of the N cells are calculated from the values of H and utilized for the free surface SLIC and cell labeling (Fig. 2 left) [8–10].

Then, the free surface is anew, more accurately reconstructed using also inclined line segments at 45° , e.g. for the middle S cells in the following diagonal configurations of surface cells:

$$\begin{array}{ccc} \text{S} & & \text{S} \\ \text{S} & (\text{Fig. 2 left}) \text{ and} & \text{S} \\ \text{S} & & \text{S} \end{array}, \text{ respectively.}$$

The TLIC is performed by a conservatively redistributing of the VOF fractions as follows.

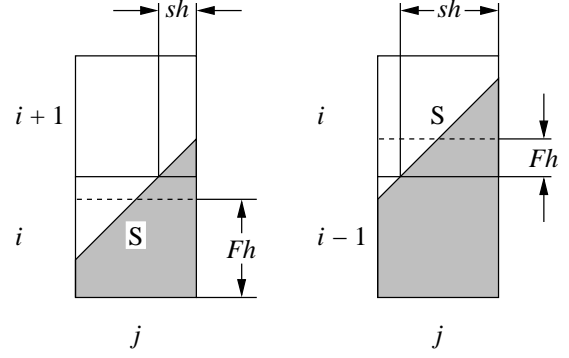


Fig. 5. Concerning the VOF fraction redistribution.

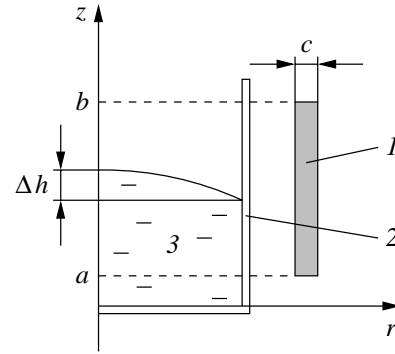


Fig. 6. Transverse section of test furnace (schematic). 1 – inductor, 2 – crucible, 3 – melt.

If for the considered surface cell i, j in a column j $F \geq 0.5$ (**Fig. 5** left), then, when using an uniform grid

$$s = F - \frac{1}{2}, \quad F_{i+1,j} = \frac{1}{2}s^2, \quad (16)$$

$$F_{i,j} = 1 - \frac{(1-s)^2}{2}.$$

If for the S cell $F < 0.5$ (**Fig. 5** right), then

$$s = F + \frac{1}{2}, \quad F_{i,j} = \frac{1}{2}s^2, \quad (17)$$

$$F_{i-1,j} = 1 - \frac{(1-s)^2}{2}.$$

6. RESULTS

The MFD field was simulated in a test ICF (**Fig. 6**) described in **Table 2** [11, 12], using the k - ϵ model. By partially filling the nonmagnetic steel crucible with molten Wood's metal, an intensive turbulent flow was electromagnetically driven in the laboratory furnace [12], which is suitable for experimental verifications of flow calculations.

By applying the FDM for a 40×120 grid in the r - and z -directions, the developed SOLA-VOF method – combined with a generalized LHF and a TLIC – was implemented in a self-developed computational program for two-dimensional (2D) MFD simulations.

In calculation of the MFD field, the inductor was considered to be fed at time $t \geq 0$ with a sinusoidal current of constant r.m.s. value I (Table 2).

Table 2. Characteristics of the ICF (Fig. 6) [11, 12]

supply frequency, r.m.s. value of the inductor current	$f = 386 \text{ Hz}$ $I = 2 \text{ kA}$
number of inductor's series turns	$n = 11$
inner diameter of inductor	385 mm
inferior and superior heights of the copper tube inductor	$a = 47.5 \text{ mm}$ $b = 570 \text{ mm}$
wall thickness of the copper tube	$c = 3.5 \text{ mm}$
inner diameter of crucible	316 mm
mean height of Wood's metal melt	400 mm
physical properties of molten Wood's metal	9.4 kg/dm^3 $\sigma = 1 \text{ MS/m}$ $\mu = 4.2 \text{ cP}$ $\gamma = 0.46 \text{ N/m}$

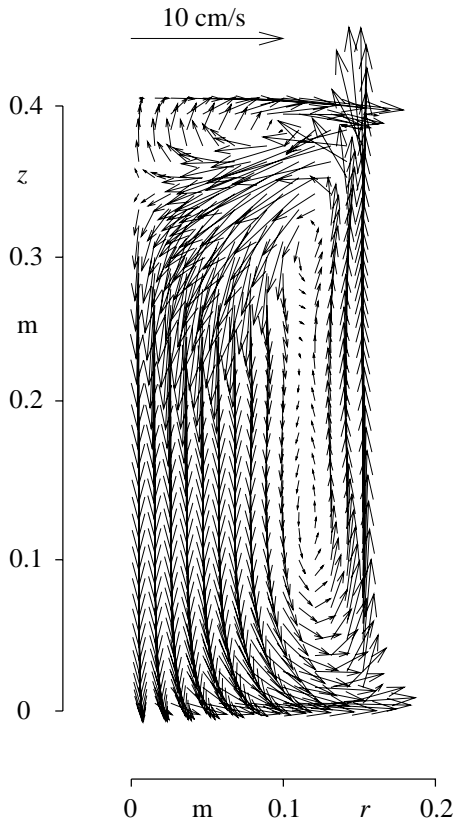


Fig. 7. Calculated velocity distribution at $t = 20 \text{ s}$.

In Fig. 6, I represents the inner walls of the inductor's copper tube with rectangular profile, only. The equation of the complex magnetic vector potential was computed assuming that the total current nI of the inductor is distributed over the area $(b - a)c$ with a density of 12 A/mm^2 .

The steady flow, determined in the MFD simulation as the final solution at $t = 20 \text{ s}$ of the transient flow, is characterized, as in the measurements [12], by one very large eddy (**Fig. 7**).

An experimental validating of accuracy in the free surface calculation was obtained as follows.

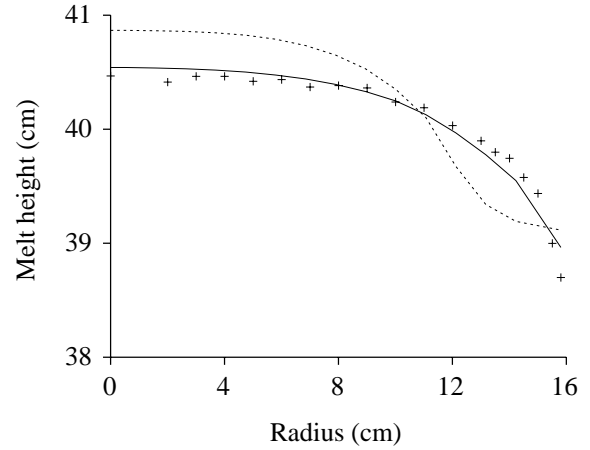


Fig. 8. Free surface profile in the ICF.

- Symbols – measured values [12]
- Solid line – calculated curve at $t = 20 \text{ s}$ by using the electrical conductivity σ of melt in all S cells
- Dotted line – calculated curve at $t = 20 \text{ s}$ by using the reduced electrical conductivity $F\sigma$ in S cells

From the visually determined melt heights using a contact method (**Fig. 8**) [12], results a bath level difference Δh (Fig. 6) of the strongly deformed free surface in the partly filled crucible of $\Delta h = 17.5\text{--}18 \text{ mm}$.

By utilization of the commercial ANSYS package for the 2D computation of the steady electromagnetic field, Lorentz forces, flow field and free surface by applying the stationary $k\text{-}\epsilon$ model as well as the classical VOF method, wavy surface shapes were calculated in [12] with a deformation of about $\Delta h = 7 \text{ mm}$, which is more than two times lower comparing to the experimentally measured height difference.

With the presented MFD simulation, implemented with the unsteady $k\text{-}\epsilon$ model in the self-developed computer program, a smooth free surface profile with a more accurately calculated bath level difference of $\Delta h = 15.8 \text{ mm}$ was determined (Fig. 8).

Fig. 8 also shows the wrong surface shape computed by using the usually reduced electrical conductivity $F\sigma$ in S cells instead of the whole melt conductivity σ employed in this study. The lines in Fig. 8 were drawn by joining the middle points of the line segments resulted from the free surface TLIC.

7. REFERENCES

- [1] C.W. Hirt, and B.D. Nichols, "Volume of Fluid (VOF) Method for Dynamics of Free Boundaries," *J. Comp. Phys.*, vol. 39, pp. 210–225, 1981.
- [2] B.D. Nichols, and C.W. Hirt, "Improved free surface boundary conditions for numerical incompressible-flow calculations," *J. Comp. Phys.*, vol. 8, pp. 434–448, 1971.
- [3] W.F. Noh, and P. Woodward, "SLIC (simple line interface calculation)," in *Lecture Notes in Physics*,

Proc. Fifth Int. Conf. on Numer. Meth. Fluid Dynamics, vol. 59, A.I. van de Vooren, and P.J. Zandbergen, eds., Springer, New York, pp. 330–340, 1976.

[4] M. Rudman, “Volume-tracking methods for interfacial flow calculations,” *Int. J. Numer. Meth. Fluids*, vol. 24, pp. 671–691, 1997.

[5] W.J. Rider, and D.B. Kothe, “Reconstructing volume tracking,” *J. Comp. Phys.*, vol. 141, pp. 112–152, 1998.

[6] P. Liovic, J.-L. Liow, and M. Rudman, “A volume of fluid (VOF) method for the simulation of metallurgical flows,” *ISIJ Int.*, vol. 41, pp. 225–233, 2001.

[7] Z.A. Sabeur, J.E. Cohen, J.R. Stephens, and A.E.P. Veldman, “Investigation on free surface flow oscillatory impact pressures with the Volume of Fluid method,” in *Numer. Meth. Fluid Dynamics VI*, M.J. Baines, ed., Will Print, Oxford, pp. 493–498, 1998.

[8] J. Gerrits, Dynamics of liquid-filled spacecraft, Ph.D. Thesis, University of Groningen, 2001.

[9] K.M.T. Kleefsman, Water impact loading on offshore structures, Ph.D. Thesis, University of Groningen, 2005.

[10] K.M.T. Kleefsman, G. Fekken, A.E.P. Veldman, B. Iwanowski, and B. Buchner, “A Volume-of-Fluid based simulation method for wave impact problems,” *J. Comp. Phys.*, vol. 206, pp. 363–393, 2005.

[11] E. Baake, Grenzleistungs- und Aufkohlungsverhalten von Induktions-Tiegelöfen, VDI, Düsseldorf, 1994.

[12] M. Kirpo, Modeling of turbulence properties and particle transport in recirculated flows, Ph.D. Thesis, University of Latvia, Riga, 2008.

[13] C.-W. Chen, and W.-S. Hwang, “A modified free surface treatment for the modeling of puddle formation in planar flow casting process,” *ISIJ Int.*, vol. 35, pp. 393–401, 1995.

[14] M. Griebel, T. Dornseifer, and T. Neunhoffer, Numerische Simulation in der Strömungsmechanik, Vieweg, Braunschweig, 1995.

[15] U. Brockmeier, Numerisches Verfahren zur Berechnung dreidimensionaler Strömungs- und Temperaturfelder in Kanälen mit Längswirbelerzeugern und Untersuchung von Wärmeübergang und Strömungsverlust, Ph.D. Thesis, Ruhr University of Bochum, 1987.